

Research Article

Genjie Chu, Sijia Li, Jiyun Gao, Li Yang*, Ming Hou*, and Shenghui Guo

Evolution of surface morphology and properties of diamond films by hydrogen plasma etching

<https://doi.org/10.1515/gps-2022-8110>

received September 14, 2022; accepted December 02, 2022

Abstract: The micron-scale diamond film was prepared using hydrogen and methane as the mixed gas supplies via self-developed 3 kW/2,450 MHz microwave plasma chemical vapor deposition (MPCVD) equipment. On this basis, the evolution of the surface morphology, hydrophobicity, and electrical properties of samples under different hydrogen plasma etching times was investigated. The results indicate that the crystal edge and the top of the diamond grain were preferentially etched when etching time is less than 30 min. The surface roughness reduced from 0.217 to 0.205 μm , and the resistance value decreases from 3.17 to 0.35 $\text{M}\Omega$. However, as the etch time increases to 120 min, the etching depth increases, and the surface roughness was increased. Simultaneously, the contact angles increased from 62.8° to 95.9°, which indicates that the surface of the diamond films exhibits more pronounced hydrophobicity. The treatment time of hydrogen plasma has no significant effect on the resistance value in the range of 0.26–0.50 $\text{M}\Omega$. The mechanism of surface etching by hydrogen plasma was also discussed.

Keywords: microwave plasma chemical vapor deposition, diamond film, surface treatment, hydrogen plasma

1 Introduction

The diamond is a crystalline material composed of a carbon atom. It belongs to the equiaxial crystal system, and the crystal structure is face-centered cubic. Diamond's unique crystal structure determines its excellent physical and chemical properties [1]. Since natural diamonds come in a wide variety of shapes, it is not easy to apply them in practical applications. The excellent properties of chemical vapor deposition (CVD) diamond films are similar to natural diamond such as high thermal conductivity, high stability, and superhardness. Therefore, the CVD diamond has been studied widely in recent years [2–4]. With the further development of diamond technology in the field of optics, electricity, and acoustics, the requirements for surface morphology and flatness control will be more stringent [5–7]. In addition to surface flatness and damage control techniques [8], the diamond surface bond state also determines its practical application. At the same time, surface wettability is directly related to the application area of diamond film. For example, biological cells require hydrophilic surfaces for adhesion and growth; conversely, diamond coatings used to protect equipment from chemical attacks require hydrophobic films [9]. Moreover, if the high resistance problem of the diamond film can be improved, it can also be better developed in the semiconductor field.

Currently, mechanical polishing and plasma treatment techniques are mainly used to control the diamond surface. The mechanical polishing process is inefficient and prone to processing damage [10]. Up to now, plasma etching is the primary and most effective method for diamond surface morphology and bond state modulation. Plasma etching technique is to precisely control the sample by sputtering, reactive ions, high-density plasma, etc., in the presence of ions. The advantages of this method are fast reaction rate, low pollution, readily adjustable auxiliary gas, and process parameters. However, this method also has certain disadvantages, such as preferential etching of grain boundaries of diamond films, plasma etching rate is slow, and etched surface flatness is difficult to control, etc. [11]. The diamond can

* Corresponding author: Li Yang, Faculty of Metallurgical and Energy Engineering, Kunming University of Science and Technology, Kunming 650093, China, e-mail: yanglikmust@163.com

* Corresponding author: Ming Hou, Faculty of Metallurgical and Energy Engineering, Kunming University of Science and Technology, Kunming 650093, China, e-mail: houmingkmust@163.com

Genjie Chu, Sijia Li: State Key Laboratory of Complex Nonferrous Metal Resources Clean Utilization, Faculty of Metallurgical and Energy Engineering, Kunming University of Science and Technology, Kunming, 650093, China

Jiyun Gao: School of Chemistry and Environment, Yunnan Minzu University, Kunming 650093, China

Shenghui Guo: Faculty of Metallurgical and Energy Engineering, Kunming University of Science and Technology, Kunming 650093, China

form a carbon–hydrogen bonding state on the surface after hydrogen plasma treatment. This bond state enables the diamond with a p-type conductive. Studies show that diamond surface carbon–hydrogen bonding state has high conductivity, stability, and corresponding device performance [12–19]. However, the surface of a diamond becomes rough due to excessive plasma etching time in the hydrogen terminal formation process, which severely affects the performance of hydrogen terminal diamond and its related electronic devices. As a result, controlling the flatness of the diamond surface and the carbon–hydrogen bonding state is particularly important for hydrogen terminal diamond applications.

In this article, the effect of different hydrogen plasma etching times on the micron-scale diamond film is studied. The surface morphology and roughness of diamond films are characterized by a scanning electron microscope (SEM) and an atomic force microscope (AFM). The effect of hydrogen plasma etching on the wettability of diamond surface is investigated by angle contact measuring device. Finally, the effects of etching on the diamond surface conductivity are characterized by four-probe resistance tester.

2 Experimental section

2.1 Preparation of high-quality micron-scale diamond film

The single-sided polished silicon wafer (2.54 cm × 2.54 cm, 100-oriented, p-type) was used as a starting substrate. Before the preparation of diamond, the silicon substrate was first mechanically polished and sonicated. The surface of the substrate creates a uniform scratch by pretreatment. These scratches will provide growth spots for polycrystalline diamond growth. Pretreatment can not only shorten the nucleation time but also effectively improve the nucleation density of diamond film [20]. The first step of diamond

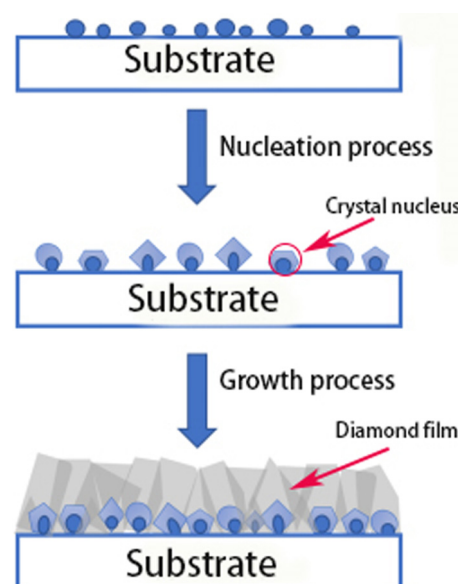


Figure 1: Schematic diagram of diamond grain growth.

growth is the nucleation process, which directly affects the quality of diamond. Therefore, in addition to substrate type and pretreatment method, nucleation parameters are also very important. Adopt self-developed 3 kW/2,450 MHz microwave plasma chemical vapor deposition (MPCVD) device. The nucleation was performed for 1 h with a microwave power of 1,700 W, a hydrogen flow rate of 400 sccm, a methane flow rate of 12 sccm, a gas pressure of 12 kPa, and a temperature of 700°C.

Diamond nucleation lays a good foundation for the subsequent growth of high-quality diamond film, while the growth of diamond film is more important. Figure 1 shows the process of the growth of polycrystalline diamond, the grains gradually grow up and contact with each other, and grains were changed from transverse to longitudinal growth [21]. The growth parameters are as follows: microwave power is 2,200 W, methane/hydrogen ratio is 2.4%, gas pressure is 14 kPa, and diamond is grown at 850°C for 4 h. The thickness of the grown micron diamond film is about 6–10 μm.

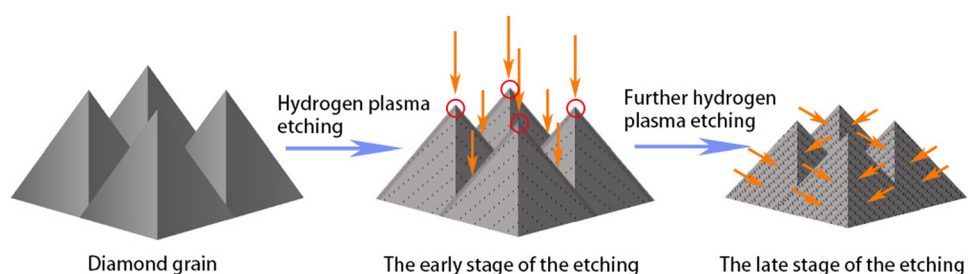


Figure 2: Plasma etching diamond film flattening process schematic.

2.2 Hydrogen plasma etching

The surface of the micron-scale diamond film has a certain roughness. Diamond films were etched with hydrogen plasma to make the (111) orientation surface flat [22,23], and Figure 2 shows the planarization schematic. The diamond films were treated with hydrogen plasma. Etching is performed in an MPCVD apparatus. The following parameters were utilized for etching: a microwave power of 2,000 W, a hydrogen flow rate of 200 sccm, a gas pressure of 10 kPa, and a temperature of 700°C. Five bunches of etching tests beneath diverse time were carried out. The etching time is 0, 30, 60, 90, and 120 min, respectively.

3 Results and discussion

3.1 Surface morphology

SEM of the prepared diamond films is shown in Figure 3. The micron-sized diamond films were prepared under the aforementioned process conditions: fast growth rate, good homogeneity, and high quality. It has a typical octahedral morphology and grain (111) preferred orientation. It demonstrates that the crystalline grains that have formed on the surface of the diamond are compact and homogeneous. The growth rate is about $1.706 \mu\text{m}\cdot\text{h}^{-1}$, and purity of the diamond phase is about 85.7% [24].

The SEM images of the diamond films before and after etching are displayed in Figure 4. The crystalline grain of the initial CVD diamond films had no visible flaws. The crystalline grains are complete and uniform (Figure 4a). After 30 min of etching, the crystalline surface has a

significant number of pits and steps (Figure 4b). The grain edges become blurry, and the grain boundaries became more evident. This kind of phenomenon can be due to adjacent position, which was more susceptible to etching. The diamond big grains collapse into tiny grains, and the graphite phase is etched by hydrogen plasma at the grain boundaries. Figure 4c shows that as the etching duration increases to 60 min, the number of etched pits on diamond grain surface increases and grain boundary deepens, the grain outline becomes more blurred, and the grain edges are more seriously etched than at 30 min of etching. When the etching time is prolonged further, the etching speed of the border of the grain increases significantly. Simultaneously, the edge of the crystal's etching is deeper, as shown in Figure 4d. When the etching time is up to 120 min, the etching is more severe at the grain boundaries, and the grain collapse tends to be flat (Figure 4e).

Electrons are known to be easily emitted from the crystal edge. The electric field increases as the number of electrons at the crystal edge rises. Therefore, the ions are not attracted to bombard the edge of the crystal because the moving electrons are suppressed to the surface of the film [25,26]. As a consequence, the crystal edge and top of the grain are preferentially etched during the early stages of hydrogen plasma treatment [27]. The non-diamond phases at the diamond grains and grain boundaries are etched by hydrogen plasma, and the depth of grain boundaries increases significantly. At this point, it is also fastest collapse of the diamond grains. Etching becomes more concentrated on the grain boundary as the etching duration increases. Although the degree of edge etching is still increasing significantly and further collapse of grains has occurred, the morphological changes at this point are less than those at the early stage of the etching. This is due to the hydrogen plasma's etching rate on graphite phase, which is approximately 50 times higher than that on diamond phases. So, graphite phase in the early stage of the etching was removed. The formation of CH and C₂ groups during etching proves that hydrogen plasma interacts with C atoms on the diamond surface. The reaction kinetics during etching proved faster etching at diamond defects [28].

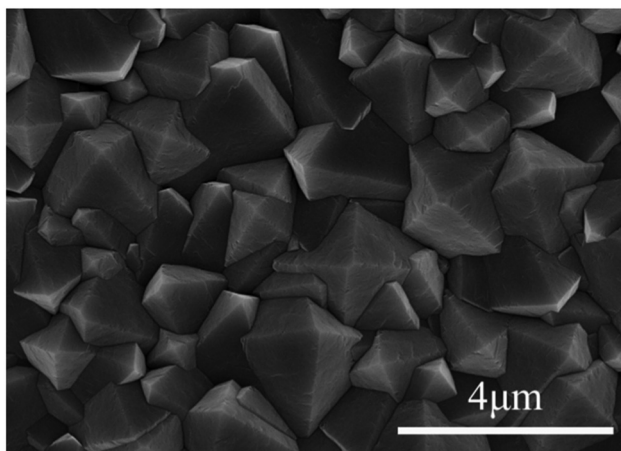


Figure 3: SEM morphology of micron-scale diamond film surface.

3.2 Surface roughness

As is shown in Figure 5, when the etching time is 0, 30, 60, 90, and 120 min, the surface roughness of the samples in the $8 \mu\text{m} \times 8 \mu\text{m}$ test range is 0.217, 0.205, 0.239, 0.256, and 0.316 μm , respectively. Therefore, the roughness of

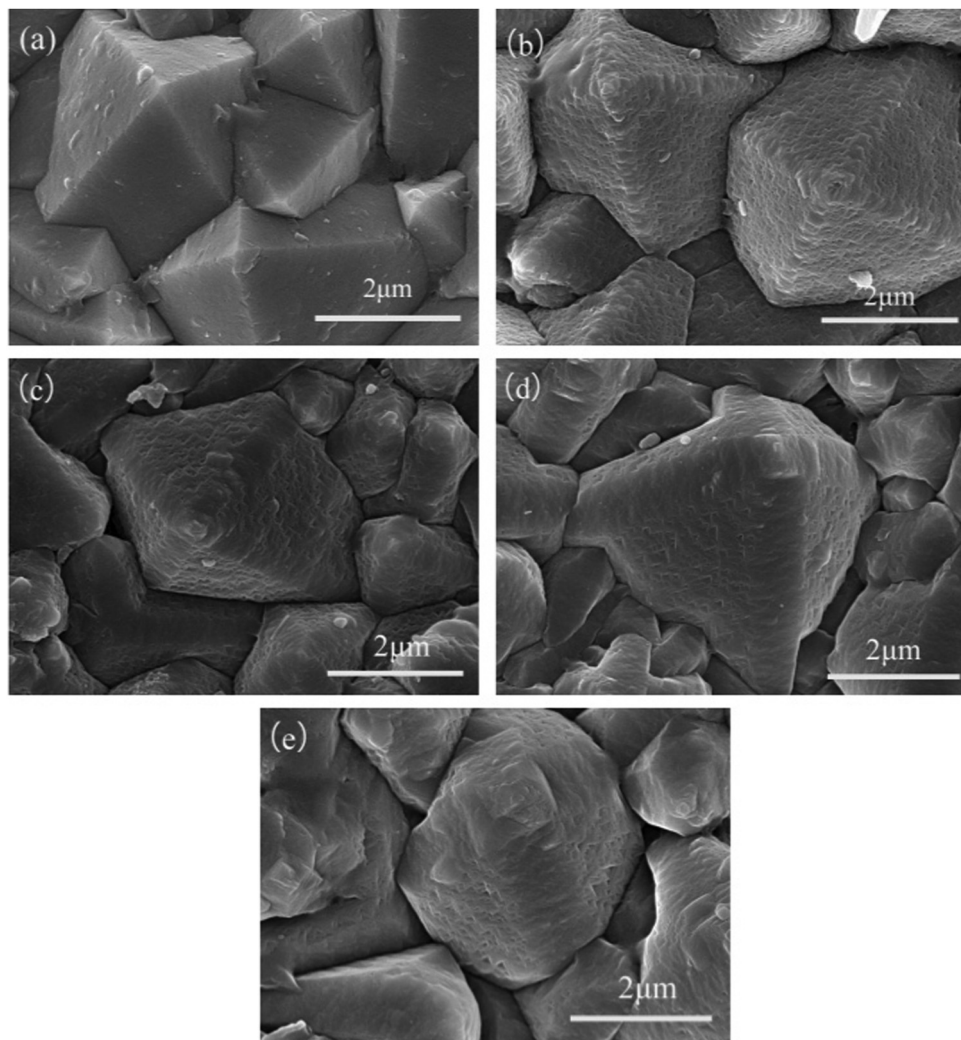


Figure 4: SEM images of samples etched at various times: (a) 0, (b) 30 min, (c) 60 min, (d) 90 min, and (e) 120 min.

the original micron diamond film is $0.217 \mu\text{m}$ (Figure 5a). After 30 min of hydrogen plasma etching, the roughness is reduced to $0.205 \mu\text{m}$ (Figure 5b). The diamond grain edges and top are severely etched. With the grain collapse into small island-shaped grains, the crystalline grains flatten somewhat. The etching speed of the top of the grain and the edge of the crystal is faster than the etching speed of the grain boundary, and it is preferentially etched in steps along the surface of the grain. Therefore, the change in grain etching effect results in the lowest surface roughness at this time. When the etching time further extends to 60 min, surface roughness of the sample is increased to $0.239 \mu\text{m}$ (Figure 5c). Although the grain boundary continues to deepen, the collapse rate of diamond grains is much lower than that in the early etching stage. With the prolongation of etching time, there is an increase in the number of etching pits. Therefore, the

surface roughness of samples has increased. When the etching time is extended 90 min, increase of etching pits on diamond surface and increase of step-like pits on grain edges. At the same time, the grain boundaries continue to deepen. The roughness increases to $0.256 \mu\text{m}$ (Figure 5d). When the etching time reaches 120 min, the largest roughness of the sample is about $0.316 \mu\text{m}$ (Figure 5e). The later stages of etching mainly show an increase in the number of craters on the grain surface, a continuous deepening of grain boundary etching, and an increase in the degree of step-like etching on the grain edges. The etching forms etching pits at defects such as dislocations, and the anisotropic effect of grain etching also comes out gradually.

The relationship between sample roughness and etching time shows that plasma etching increases the surface roughness of the sample. As the etching time increases, the surface roughness decreases from $0.217 \mu\text{m}$ at first to $0.205 \mu\text{m}$ and

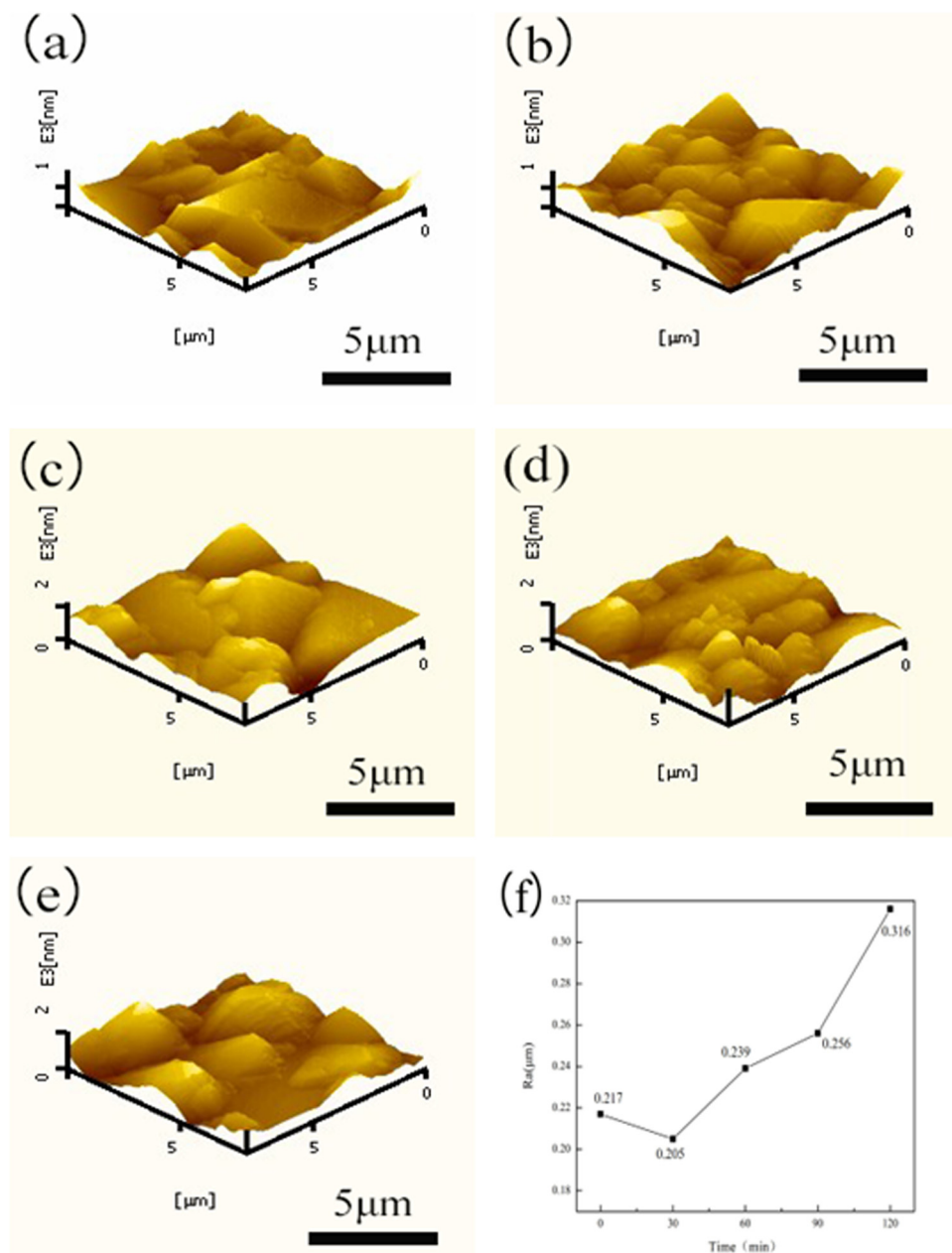


Figure 5: AFM images of samples etched at various times: (a) 0, (b) 15 min, (c) 20 min, (d) 60 min, (e) 90 min, and (f) 120 min.

finally continues to rise to 0.316 $\mu{\text{m}}$. Overall, first it showed a decreasing trend and then increased. This is consistent with SEM results.

3.3 Wettability and surface resistances

Angle contact measurement equipment was used to analyze the wettability of diamond samples before and after etching, which is illustrated in Figure 6. The contact angle of an unetched diamond sample with water is

approximately 62.8° , as shown in Figure 6a, which reflected a marked hydrophilic character. Under these process conditions, a large amount of C–O exists on the surface of the prepared micron-scale diamond film. The oxygen terminal of diamond film shows hydrophilicity. Thus, surface bonds are the main cause of hydrophilicity. When the etch time increases to 30 min, the contact angle increases to 71.2° (Figure 6b). A part of the C–O bond on the surface of diamond film changes to C–H bond, which increases the contact angle of diamond film. Diamond film surface still behaves hydrophilically. As etching time increases to

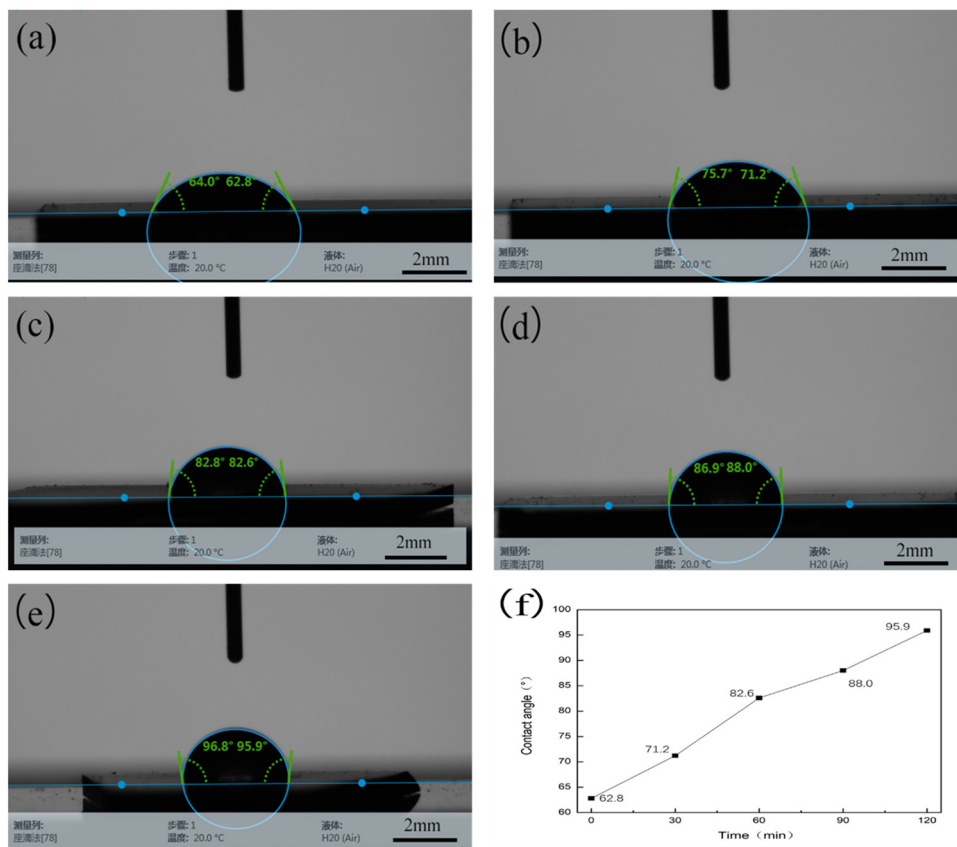


Figure 6: Diamond film contact angle test results: (a) 0, (b) 30 min, (c) 60 min, (d) 90 min, (e) 120 min, and (f) contact angle variation curve with time.

60 min, the contact angle was increased again to 82.6° (Figure 6c). The contact angle has been obviously increased compared with that before etching. As shown in Figure 6d, as the etching time increases to 90 min, the contact angle increases to 88°. Although the contact angle rises, it remains less than 90°, indicating that the diamond film surface is still hydrophilic. After etching for 120 min, the contact angle finally reaches 95.9° (Figure 6e). At this point, the surface of diamond film is hydrophobic. The hydrophilicity and hydrophobicity of the diamond film are mainly affected by the hydrogen and oxygen terminal functional groups. When the surface of diamond is oxygen terminal, the wettability appears as hydrophilic. The strong interaction between the water molecules and the terminal oxygen leads to the formation of new chemical bonds on the surface of an atom. When the surface of diamond is hydrogen terminal, it usually shows hydrophobicity. The degree of hydrophobicity is closely related to the type and number of chemical bonds on the surface.

The different bond states of carbon atoms make their surface terminal states different. After etching by hydrogen plasma, the surface of diamond film is damaged. The

formation of C–H bond gradually replaces C–O bond, and C–O bond shows strong dipolar-polarization effects [29]. Finally, the conversion of oxygen terminal to hydrogen terminal is realized. A solid surface's wettability is primarily governed by two factors: chemical composition and roughness [30]. Hence, we increase the contact angle with increasing etching time. The surface of the diamond film was turned from hydrophilic to hydrophobic.

As shown in Figure 7, the resistivity of diamond was measured by a four-probe tester. The surface resistance of the micron-scale diamond film without hydrogen plasma etching is 3.71 MΩ. As is known to all, the diamond itself is an insulating material because of the high resistance nature. High resistance greatly limited being applications in the field of semiconductive electronic device. Nevertheless, after etching, the evolution of resistance is significantly changed. As the etch time increases to 30 min, the resistance value becomes 0.35 MΩ. This is consistent with the study by Liu [31]. The decreased surface roughness in diamond films leads to enhancement of carrier–carrier scattering effect. Thus, the carrier mobility is considerably increased and the resistance decreased obviously for

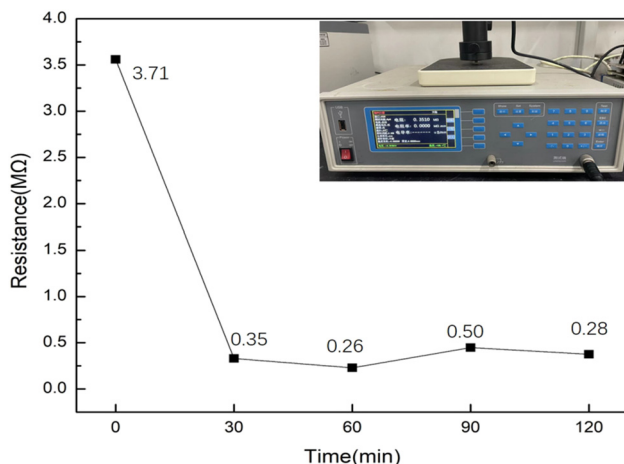


Figure 7: Micron-scale diamond film square resistance value with hydrogen plasma etching time.

diamond films. This is in a good agreement with our AFM results. This means that the hydrogen terminal is gradually forming on the diamond surface. This is consistent with the contact angle results. The square resistance did not change significantly for etching times between 30 and 120 min. Its value fluctuates at 0.26–0.50 MΩ.

The insulating diamond acquires conductive properties on the basis of hydrogen plasma treatment. The hydrogen terminal structure is formed on the surface. Combined with the analysis of wettability and surface resistance, the hydrogen-terminated diamond film after hydrogen plasma etching, the surface of which is hydrophobic, and the hydrogen-terminated surface producing dipoles, the energy required for electrons to be pulled out is reduced, and diamond film surface with negative electron affinity can interact with external receptors. The surface of diamond material loses electrons and forms P-type semiconductor hole orbits [32]. The surface resistance is reduced, and the conductivity is enhanced. Therefore, less than 30 min of etching time leads to an increase in carrier mobility. At this moment, the hydrogen terminal diamond can be realized semiconducting without ion implantation or doping.

4 Conclusion

In this article, the effects of hydrogen plasma treatment on the surface morphology and properties of micron diamond were characterized by SEM, AFM, contact angle tester, and four-probe resistance tester. The following conclusions are obtained.

In the prophase of etching, the electric field increases as the number of electrons at the crystal edge grows. The

motion of electrons toward the surface of diamond films in the plasma is suppressed, and ions are attracted to bombard the edges of the crystal. Therefore, the crystal edge and the top of the grain are preferentially etched, and the surface roughness reduced. But when the etching duration exceeds 30 min, etching is mainly concentrated on the grain boundary. The outline of the grains became blurry, and the crystalline surface has a significant number of pits and steps. At the same time, the roughness slowly increases.

The contact angle also increases from 62.8° to 95.9° with the increase in etching time. The surface of the diamond film was turned from hydrophilic to hydrophobic. This is because the surface of the diamond film is destroyed following etching, and the formation of C–H bond gradually replaces C–O bond. Finally, the conversion of oxygen terminal to hydrogen terminal is realized.

The reduction in surface roughness of the diamond film 30 min before etching leads to the enhancement of carrier scattering effect. As a result, the carrier mobility of the diamond film is greatly increased, increases the H on the diamond film surface, slightly decreases the wettability, increases the surface roughness, and decreases the surface resistance to 0.35 MΩ. However, the resistance of the diamond film does not change significantly by extending the etching time and remains at 0.26–0.50 MΩ. Therefore, the factors affecting the surface resistance are multiple and need to be considered in a comprehensive manner.

Funding information: This research was funded by the National Natural Science Foundation of China (No. 51864028), Yunnan Province Science and Technology Major Project for Materials Genetic Engineering of Rare and Precious Metal (No. 202002AB080001), Yunnan Province Funds for Distinguished Young Scientists (No. 2019FJ005), and Science Research Foundation of Yunnan Provincial Education Department (No. 2022J0441).

Author contributions: Genjie Chu: writing – original draft, writing – review and editing, formal analysis; Sijia Li: writing – original draft, formal analysis; Jiyun Gao: visualization, project administration; Li Yang: supervision, conceptualization, writing – reviewing and editing; Ming Hou: methodology, formal analysis; Shenghui Guo: resources.

Conflict of interest: Authors state no conflict of interest.

Data availability statement: All data generated or analyzed during this study are included in this published article.

References

- [1] Srikanth VS. Review of advances in diamond thin film synthesis. *Proc Inst Mech Eng C J Mech Eng Sci.* 2012;226(2):303–18.
- [2] Shen XT, Wang XC, Sun FH, Ding CY. Sandblasting pretreatment for deposition of diamond films on WC-Co hard metal substrates. *Diam Relat Mater.* 2017;73:7–14.
- [3] Li X, Ye JS, Zhang HC, Feng T, Chen JQ, Hu XJ. Sand blasting induced stress release and enhanced adhesion strength of diamond films deposited on austenite stainless steel. *Appl Surf Sci.* 2017;412:366–73.
- [4] Wang XC, Wang CC, Shen XT, Sun FH. Tribological properties of diamond films for high-speed drawing Al alloy wires using water-based emulsions. *Tribol Int.* 2018;123:92–104.
- [5] Faycal HL, Rafik SS. SAW devices: Review of numerical-experimental studies and recent applications. *Sens Actuator A Phys.* 2019;292(6):169–97.
- [6] Castelletto S, Rosa L, Blackledge J, Abri MZ, Boretti A. Advances in diamond nanofabrication for ultrasensitive devices. *Microsyst Nanoeng.* 2017;3(10):1–16.
- [7] Lee JC, Magyar AP, Bracher DO, Aharonovich L, Hu EL. Fabrication of thin diamond membranes for photonic applications. *Diam Relat Mater.* 2013;33(3):45–8.
- [8] Wort CJH, Balmer RS. Diamond as an electronic material. *Mater Today.* 2008;11(1–2):22–8.
- [9] Montaño-Figueroa AG, Alcantar-Peña JJ, Tirado P, Abraham A, Obaldia ED, Auciello O. Tailoring of polycrystalline diamond surfaces from hydrophilic to superhydrophobic via synergistic chemical plus micro-structuring processes. *Carbon.* 2018;139:361–8.
- [10] Zheng YT, Ye HT, Thornton R, Knott T, Ochalski TJ, Wang J, et al. Subsurface cleavage of diamond after high-speed three-dimensional dynamic friction polishing. *Diam Relat Mater.* 2020;101:107600.
- [11] Toros A, Kiss M, Graziosi T, Mi S, Berrazouane R, Naamoun M. Reactive ion etching of single crystal diamond by inductively coupled plasma: State of the art and catalog of recipes. *Diam Relat Mater.* 2020;108:107839.
- [12] Sque SJ, Jones R, Öberg S. Transfer doping of diamond: Buckminsterfullerene on hydrogenated, hydroxylated, and oxygenated diamond surfaces. *J Mater Sci Mater Electron.* 2006;17:459–65.
- [13] Jiang CY, Guo SH, Gao JY, Hu T, Yang L, Peng JH, et al. Optimization of growth parameters for diamond films grown by MPCVD using response surface methodology. *Arab J Sci Eng.* 2016;41:2671–80.
- [14] Sachin B, Narendranath S, Chakradhar D. Application of desirability approach to optimize the control factors in cryogenic diamond burnishing. *Arab J Sci Eng.* 2020;45:1305–17.
- [15] Yamanaka S, Ishikawa K, Mizuochi N. Structural change in diamond by hydrogen plasma treatment at room temperature. *Diam Relat Mater.* 2005;14:6095–9.
- [16] Verona C, Arciprete F, Foffi M. Influence of surface crystal-orientation on transfer doping of V_2O_5 /H-terminated diamond. *Appl Phys Lett.* 2018;112:181602.
- [17] Ren ZY, Lv DD, Xu JM. High temperature (300°C) ALD grown Al_2O_3 on hydrogen terminated diamond: Band offset and electrical properties of the MOSFETs. *Appl Phys Lett.* 2020;116:013503.
- [18] Inaba M, Kawarada H, Ohno Y. Electrical property measurement of two-dimensional hole-gas layer on hydrogen-terminated diamond surface in vacuum-gap-gate structure. *Appl Phys Lett.* 2019;114:253504.
- [19] Kasu M, Ueda K, Yamauchi Y. Diamond-based RF power transistors: Fundamentals and applications. *Diam Relat Mater.* 2007;16(1):1010–5.
- [20] Huang JL, Wang JH. Nucleation study of CVD diamond films. *Mater Direct.* 2007;2:312–5.
- [21] Zhu HX, Mao WM, Feng HP, Lv RX, Vlasov II. Effect of methane concentration on the crystallographic growth process of CVD diamond films. *J Inorg Mater.* 2007;3:570–6.
- [22] Song J. Preparation and optical properties of gold nanoparticles/diamond composite structures. *Changchun: Journal of Jilin University;* 2015.
- [23] Jacek J. Densely packed tetrahedra clusters displaying diamond-like superstructures. *Particuology.* 2021;58:147–52.
- [24] Feng SG. Preparation of diamond film by MPCVD method and its surface treatment process. *Kunming: Kunming University of Science and Technology;* 2021.
- [25] Pan X, Ma ZB, Li GW. Mechanism of etching CVD diamond film by oxygen plasma. *High Power Laser Part Beams.* 2014;26(7):243–7.
- [26] Wu J, Ma Z, Shen W. Effect of nitrogen in CVD diamond on plasma etching. *Acta Phys Sin.* 2013;62(7):262–8.
- [27] Hayashi K, Yamanaka S, Okushi H, Kajimura K. Stepped growth and etching of (001) diamond. *Diam Relat Mater.* 1996;5(9):1002–5.
- [28] Yurov V, Bushuev E, Bolshakov A, Ashkinazi E. Etching kinetics of (100) single crystal diamond surfaces in a hydrogen microwave plasma, studied with *in situ* low-coherence interferometry. *Phys Status Solidi A.* 2017;214(11):1700177.
- [29] Maier F, Ristein J, Ley L. Electron affinity of plasma-hydrogenated and chemically oxidized diamond (100) surfaces. *Phys Rev B.* 2001;64(16):165411.
- [30] Balu B, Breedveld V, Hess DW. Fabrication of “Roll-off” and “Sticky” superhydrophobic cellulose surfaces via plasma processing. *Langmuir.* 2008;24(9):4785–90.
- [31] Liu JL. Study on the Conductive Properties of Hydrogen-Terminated Self-Supported Diamond Film Surface and its Device Development. *Beijing: University of Science and Technology Beijing;* 2013.
- [32] Gei MW, Wade TC, Wuorio CH. Progress toward diamond power field-effect transistors. *Phys Status Solidi (A) Appl Mater Sci.* 2018;215(22):SI.